Hysteresis Flip Effects On the DC Plasma Discharge Characteristics Of A Co-Axial Electrode Geometry

Rahul Kumar[2], Ramesh Narayanan[1], R. D. Tarey[2] and A Ganguli[1]

[1]*Centre for Energy Studies, Indian Institute of Technology Delhi, Hauz Khas, New Delhi-110016, India*
[2]*Department of Physics, Indian Institute of Technology Delhi, Hauz Khas, New Delhi-110016, India*

It has been observed that there is a flip of the hysteresis in the I_d-V_d characteristics of dc plasma in coaxial electrode geometry, under two different operating conditions. A major change in the condition is observed to be the associated difference in the evolution of the floating potential oscillations as the system transits from order-to-chaos-to-order between two Negative Differential Resistance (NDR) regions. The change in the condition seems to be associated with the point at which the 1st NDR is seen to be triggered and also defines the evolution of the discharge characteristics itself subsequently.

1. Introduction

Plasma discharges being a nonlinear medium, observations of associated hysteresis effects at negative differential resistance (NDR) regions are signatures of the nonlinear dynamical evolution of the system. Such hysteresis loops are quite commonly observed near the Townsend breakdown and abnormal glow discharge regions of a planar electrode dc plasma discharge. However, there have also been observations of NDR regions in discharge current (I_d) – discharge voltage (V_d) characteristics in systems such as the DP machine [1] and coaxial electrode geometry systems [2, 3], in which the dynamical evolution of the system has been characterized using fluctuation signals [2-6] obtained from the plasma. In different systems and under different operating conditions, the fluctuation signals have been observed to undergo order-to-chaos [7] as well as chaos-to-order [8, 9] transitions.

Recently, observations of order-to-chaos-to-order transitions have also been reported [3, 10]. In a study by Kumar *et. al.* [3], the associated order-to-chaos-to-order transitions have been correlated to a hysteresis in the amplitude of the floating potential fluctuations also. The fluctuations show a characteristic change from low amplitude, high frequency oscillations to large amplitude, low frequency oscillations.

But the evolution of this low amplitude, high frequency oscillations to large amplitude, low frequency oscillations is seen to depend on the path that the I_d-V_d characteristics evolves under the same operating pressure. This behaviour of the plasma discharge is being reported in this paper.

2. Experimental Results and Discussions

Plasma discharges have been initiated in a coaxial electrode system (Material SS304, ≈6 cm long), with the central axial rod (diameter ≈ 0.15 cm) being the powered anode and the outer cylindrical tube acting as the grounded cathode, the details of which is shown in Ref [3]. Plasma measurements have been made using a single Langmuir probe.

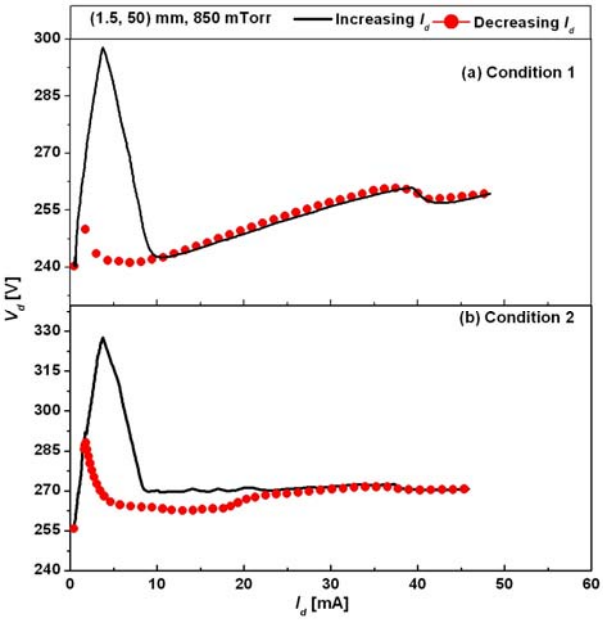

Fig 1: I_d-V_d discharge characteristics for increasing (black) and decreasing (red) I_d for two conditions (a) Condition 1 (b) Condition 2 for p=850 mTorr.

The I_d-V_d characteristics [3] are seen to have two consecutive negative differential regions (NDR) at operating pressures p ~ 750 mTorr - 950 mTorr. These NDR regions are not observed when the anode and cathode are interchanged. The 1st NDR (at about 3-7 mA) is seen to be associated with a voltage threshold. The discharge transition near the 1st NDR is observed to be quite sudden whereas the transition at the 2nd NDR is more gradual. The 1st NDR has been observed to be correlated to an upper

voltage threshold whereas the 2nd NDR is seen to be linked to the discharge current, which increases with increasing operating pressure [11].

The upper voltage threshold does seem to be dependent on the plasma discharge conditions, since with operation of the discharge over long periods of time (~ a month or two), one observes that under similar initial discharge parameters, the discharge characteristics change. This evolution is seen to repeat itself, if one re-starts the experiments with cleaner electrode surfaces. The voltage drop across this 1st NDR, does not seem to vary much (ΔV_d~ 50-60V), as observed in Fig 1(a) and Fig 1(b). Herein the former is when discharge operation has been initiated the first time (termed Condition 1, henceforth), and the latter is when the discharge operation has occurred over a significant amount of time (henceforth termed Condition 2).

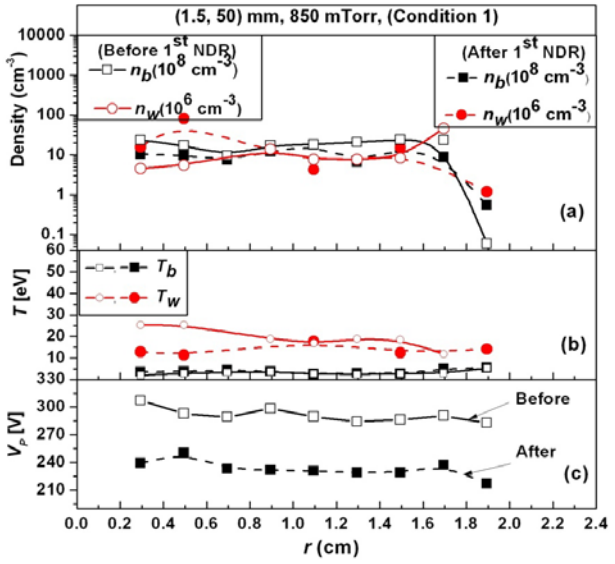

Fig 2: Plasma profiles for Condition 1 (a) bulk density (n_e) [black] and warm density (n_w) [red] (b) electron temperature (T_e) [black] and warm temperature (T_w) [red] (c) Plasma potential (V_p). The solid lines represent measurements before 1st NDR and dashed lines represent measurements after 1st NDR.

An important observation of the discharge characteristics in the two conditions seem to be related to the path that the characteristics take when I_d is being decreased. In Condition 1, the characteristic hysteresis is seen to return from the top of the forward path between the 1st and 2nd NDR whereas it is seen to return from the bottom in Condition 2. The difference in the evolution of the two conditions seems to be related to the threshold V_d at which the 1st NDR occurs, which subsequently decides the path of the discharge characteristics till the 2nd NDR. The threshold V_d for Condition 1 occurs at about 290 – 295 V. This voltage threshold is observed to shift to higher values with plasma exposure time (~295 V to ~325 V from condition 1 to condition 2 in Fig 1).

Another interesting observation in comparison of these discharges, are that in Condition 1, the discharge characteristics evolves beyond the first NDR with a positive differential resistance (PDR) whereas in Condition 2 the differential resistance in this region is almost zero. It is to be noted though that V_d at which the 2nd NDR is triggered is ~265-270 V in both conditions.

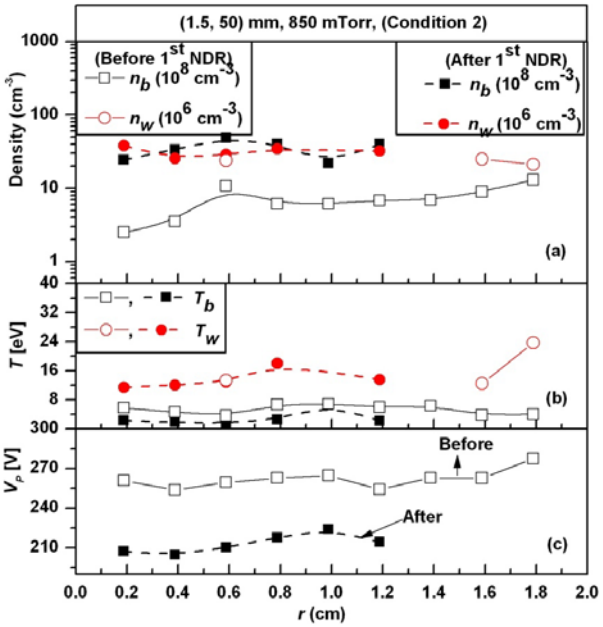

Fig 3: Plasma profiles for Condition 2 (a) bulk density (n_e) [black] and warm density (n_w) [red] (b) electron temperature (T_e) [black] and warm temperature (T_w) [red] (c) Plasma potential (V_p). The solid lines represent measurements before 1st NDR and dashed lines represent measurements after 1st NDR.

Measurement of the plasma profiles for both Condition 1 (Fig 2) and Condition 2 (Fig 3) show that the bulk plasma densities are of the same order (1-2 × 10^9 cm^{-3}) after the 1st NDR. However, the bulk density before the 1st NDR in Condition 2 is about an order of magnitude lower than Condition 1. In fact, there is no significant change in the bulk density after the 1st NDR in Condition 1. Another prominent role that could determine the evolution of the discharge seems to be the presence of a warm electron population with a temperature (16-25 eV) that is higher than the ionization potential of the operating gas (Argon) in Condition 1 whereas it is of the order or less than the ionization potential in

Condition 2. In fact, the presence of the warm population is seen to be restricted to localized regions across the radial extent of the discharge before the 1st NDR in Condition 2 [Fig 3(b)]. The plasma potential drop of ~ 60 V is observed before and after the 1st NDR in both conditions, with the radial variation of the plasma potential (V_p) being almost constant.

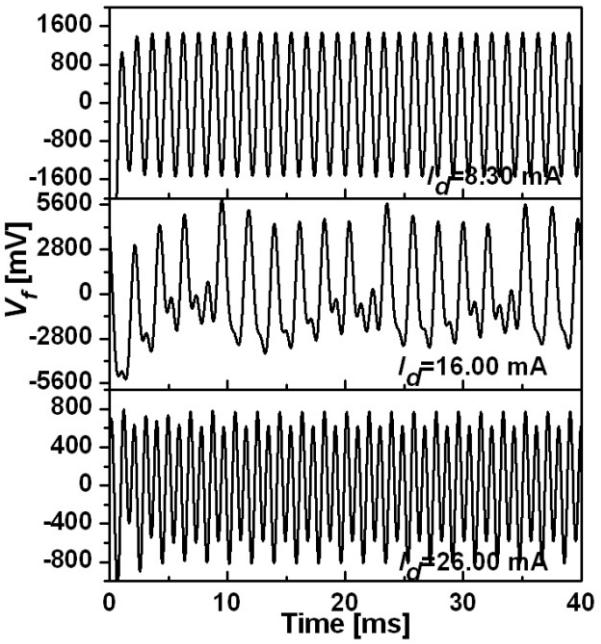

Fig. 4: Floating potential oscillations for increasing discharge current for Condition 1

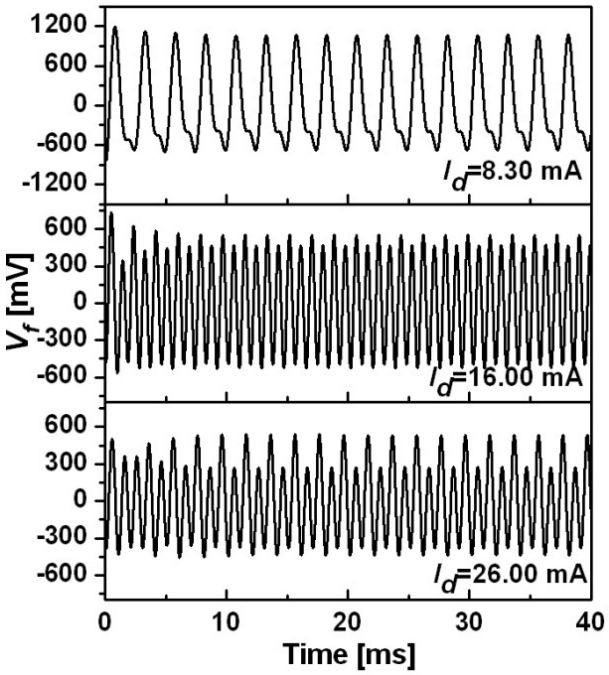

Fig. 5: Floating potential oscillations for decreasing discharge current for Condition 1

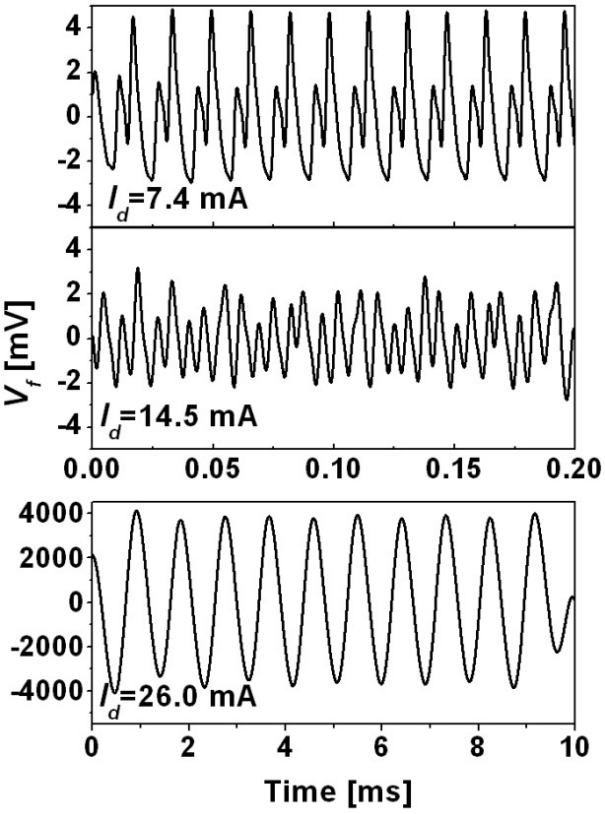

Fig. 6: Floating potential oscillations for increasing discharge current for Condition 2

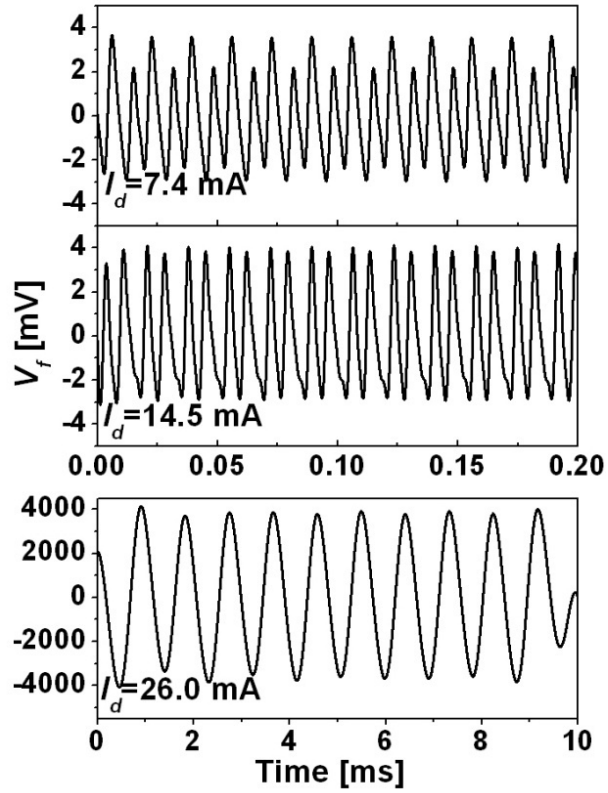

Fig. 7: Floating potential oscillations for decreasing discharge current for Condition 2

Under these operating conditions, a hysteresis is observed in the amplitudes of self-excited oscillations of the floating potential (V_f) and discharge current (I_d) [2]. This hysteresis effect is observed between the two NDR regions which occurs closer to the second NDR (I_d ~40 mA) in some conditions and in other conditions it is observed at lower I_d (~ 16-20 mA).

The evolution of the floating potential oscillations (V_f) for Condition 1 has been shown for increasing and decreasing I_d in Figs 4 and 5 respectively whereas for Condition 2 in Figs 6 and 7 respectively. In each of the figures 4-7, three typical oscillations have been depicted. The top plot in each figure represents an ordered oscillation just after the 1st NDR and then the second subplot shows a typical oscillation in the chaotic regime, wherein V_f oscillations have been seen to transit as I_d is increased. Subsequent to the transition to chaotic regime, it is observed that the oscillations transit to an ordered regime with further increase in I_d, which is depicted in the bottom plot of each figure. The three subplots in Figs. 4 and 5 are shown for I_d=8.3, 16 and 26 mA whereas in Figs 6 and 7 the oscillations at I_d=7.4, 14.5 and 26.0 mA are shown. Thus comparing the V_f plots for increasing and decreasing I_d, for each of the two conditions, one can see the existence of a hysteresis in the signals as it retraces the I_d path.

In Condition 1, the oscillation amplitudes are of the same order (~1-2 V) as the current is increased from after the 1st NDR to the 2nd NDR and back. The oscillations are observed to transit from period-1 to period-n oscillations. However, in condition 2, the initial fluctuation amplitude levels after the 1st NDR are of the order of a few mV, which then suddenly transits to amplitude levels of a few Volts. On decreasing I_d the amplitude levels return to lower levels of a few mV, with the observance of a prominent hysteresis in the amplitude levels of V_f also [3].

Another important observation is that the frequency of the oscillations in Condition 1 are in the range of 800 Hz – 2 kHz as I_d is increased from after the 1st NDR (~6-7 mA) to about 45-50 mA and then decreased back. However, in condition 2, the oscillations observed initially after the 1st NDR are in the range of a few tens of kHz and thereafter, at higher I_d, when the V_f oscillations transit to large amplitude levels, one finds that the frequency of the oscillations also decrease to ~1 kHz.

3. Conclusions

The characterization of the V_f oscillations for Condition 1 and Condition 2 have revealed the transition of low-amplitude high-frequency period-n oscillations to a large-amplitude, low-frequency period-1 oscillations through a chaotic intermediate route in case of Condition 2 which was not observed when the discharge was in Condition 1, wherein the system went into comparatively large amplitude oscillations immediately after the transition through the 1st NDR. However, the order-to-chaos-to-order transition is still seen to occur. Further the associated hysteresis in the floating potential amplitude is quite prominent only in Condition 2.

Thus it seems that the initial triggering of the discharge leading to the 1st NDR plays a significant role in the evolution of the discharge characteristics, which in turn seems to be related to the some reversible changes in the electrode surfaces properties, which now requires to be understood. Thus the evolution of the discharge characteristics in this coaxial electrode geometry is seen to depend intrinsically on the initial conditions of the discharge.

4. References

[1] C. Ionita, D. G. Dimitriu, and R. W. Schrittwieser, *Int. J. Mass. Spectrom.* **233** (2004) 343.

[2] Md. Nurujjaman, R. Narayanan, and A. N. S. Iyengar, *Chaos* **17** (2007) 043121

[3] R. Kumar, R. Narayanan and A. Prasad, *Phys. Plasmas* **21** (2014) 123501.

[4] Md. Nurujjaman and A. N. S. Iyengar, *Phy. Lett A* **360** (2007) 717.

[5] Md. Nurujjaman, R. Narayanan, and A. N. S. Iyengar, *Phys. Plasmas* **16** (2009) 102307.

[6] S. Gurlui, D. G. Dimitriu, C. Ionita, and R.W. Schrittwieser, *Rom. Journ. Phys.* **54** (2009) 705.

[7] V. Mitra , A. Sarma, M.S. Janaki, A.N. Sekar Iyenger, B. Sarma, N. Marwan, J. Kurths, P. K. Shaw, D. Saha, S. Ghosh, *Chaos, Solitons & Fractals*, 69, (2014), 285.

[8] S. Lahiri, D. Roychowdhury, and A. N. S. Iyengar, *Phys. Plasmas* **19** (2012) 082313.

[9] Md. Nurujjaman and A. N. S. Iyengar, Pramana, *J. Phys.* **67** (2006) 299.

[10] M. Agop, D. G. Dimitriu, L. Vrajitoriu, and M. Boicu, *J. Phys. Soc. Jpn.* **83** (2014) 054501.

[11] R. Narayanan, R. Kumar, R. D. Tarey and A. Ganguli, Proceedings of PPPS-2013, San Francisco, USA (July 2013), Publ. IEEE & POD Publ. Curran Associates Inc., *ISBN: **978-1-4673-5166-9,** **1,*** (2014) 435.